Superparamagnetic Iron Oxide Nanoparticles reprogram the tumor microenvironment and reduce lung cancer regrowth after crizotinib treatment

Supporting Information

Natalie K. Horvat[1,2,4*], Sara Chocarro[3,4*], Oriana Marques[1,2], Tobias A. Bauer[5], Ruiyue Qiu[1], Alberto Diaz-Jimenez[3,4], Barbara Helm[6], Yuanyuan Chen[3], Stefan Sawall[7], Richard Sparla[1], Lu Su[5], Ursula Klingmüller[6,8,9], Matthias Barz[5,10], Matthias W. Hentze[11*], Rocío Sotillo[3,8,9*#], Martina U. Muckenthaler[1,2,8,9,12*#]

1. Department of Pediatric Hematology, Oncology, Immunology and Pulmonology, Heidelberg University Hospital, Im Neuenheimer Feld 350, 69120, Heidelberg, Germany. Martina.Muckenthaler@med.uni-heidelberg.de
2. Molecular Medicine Partnership Unit (MMPU), Otto-Meyerhof-Zentrum, Im Neuenheimer Feld 350, 69120, Heidelberg, Germany.
3. Division of Molecular Thoracic Oncology, German Cancer Research Center (DKFZ), Im Neuenheimer Feld 280, 69120 Heidelberg, Germany. r.sotillo@dkfz-heidelberg.de
4. Ruprecht Karl University of Heidelberg, 69120, Heidelberg, Germany.
5. Leiden Academic Centre for Drug Research (LACDR), Leiden University, Einsteinweg 55, 2333CC, Leiden, The Netherlands.
6. Division of Systems Biology of Signal Transduction, German Cancer Research Center (DKFZ), Im Neuenheimer Feld 280, 69120, Heidelberg, Germany.
7. X-Ray Imaging and CT, German Cancer Research Center (DKFZ), Im Neuenheimer Feld 280, 69120, Heidelberg, Germany.
8. German Center for Lung Research (DZL) and Translational Lung Research Center Heidelberg (TRLC), 69120, Heidelberg, Germany.
9. German Consortium for Translational Cancer Research (DKTK), 69120, Heidelberg, Germany.
10. Department of Dermatology, University Medical Center of the Johannes Gutenberg University Mainz, Langenbeckstraße 1, 55131, Mainz, Germany.

[11] European Molecular Biology Laboratory (EMBL), Meyerhofstr.1, 69117, Heidelberg, Germany. hentze@embl.org

[12] German Centre for Cardiovascular Research (DZHK), Partner Site, 69120, Heidelberg/Mannheim, Germany.

* These authors contributed equally

Co-corresponding authors

Supplemental figure 1

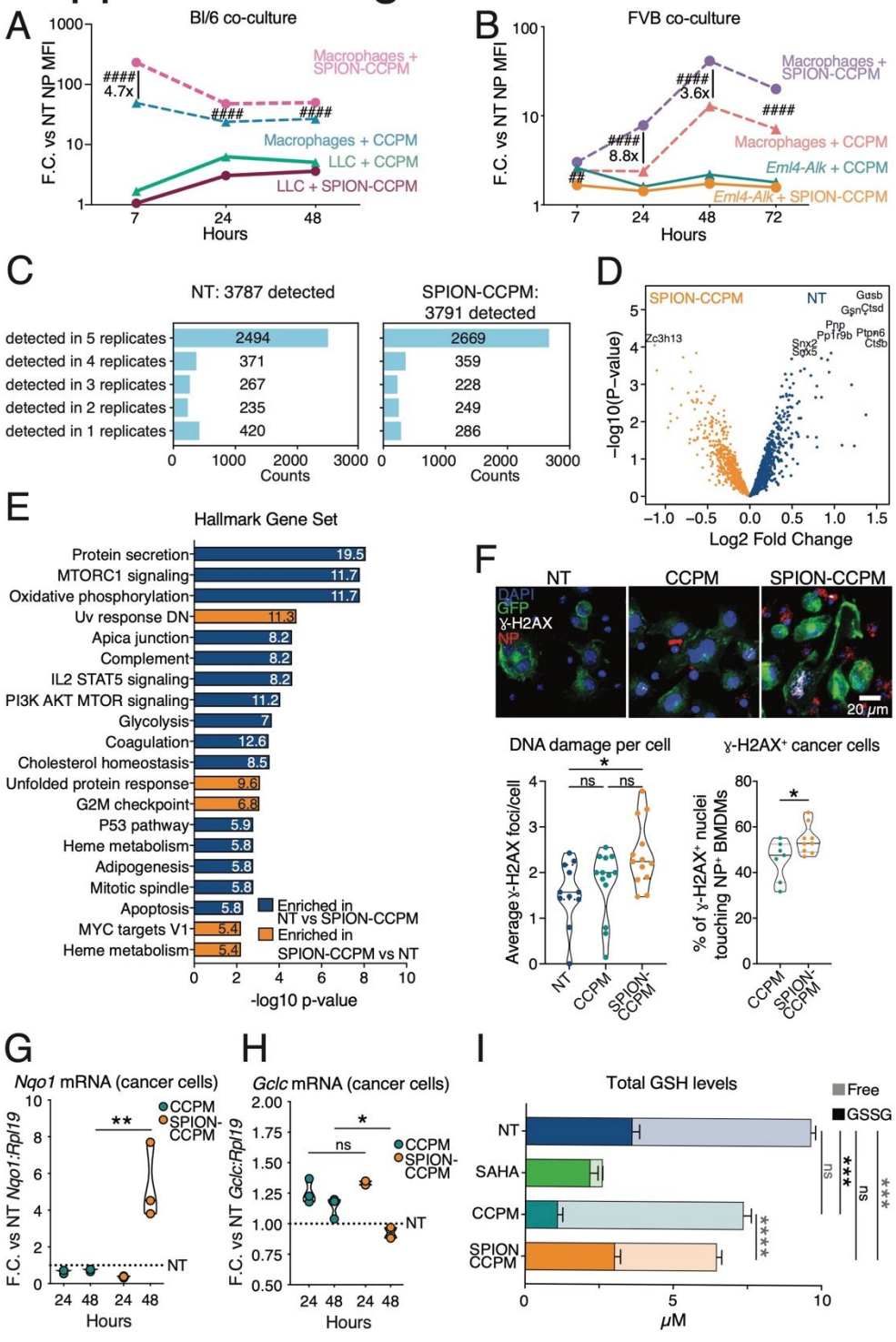

Supplemental Figure 1: SPION-CCPM-accumulation in macrophages induces oxidative stress in cancer cells

Flow cytometry measurement of nanoparticle (NP) signal intensity in Bl/6 (A) and FVB (B) co-cultured bone marrow-derived macrophages (BMDMs) with LLC (A) or *Eml4-Alk* (B) cancer cells following SPION-CCPM, CCPM or without treatment (NT); # SPION-CCPM vs CCPM. (C) Bar diagrams showing how often proteins were quantified, based on LFQ intensities, in the samples belonging to each group. (D) Volcano plot displaying the differentially regulated proteins between NT and SPION-CCPM-treated *Eml4-Alk* cells. (E) Hallmark Gene Sets of the proteome enriched in NT or SPION-CCPM *Eml4-Alk* cells co-cultured with BMDMs with indicated enrichment score. (F) γ-H2AX immunofluorescence microscopy with average foci per positive nuclei (below, left) and percent nanoparticle (NP) positive BMDMs touching γ-H2AX^{+} cancer nuclei quantification (below, right) from 2000 cells from 3 mice after 24 h of culturing. Cancer cells were endogenously labeled with GFP. mRNA expression of *Nqo1* (G) and *Gclc* (H) transcripts in co-cultured LLC cancer cells. (I) Total glutathione (GSH) levels in co-cultured *Eml4-Alk* cancer cells after 48 h treatment (NT-negative control; SAHA-positive control; CCPM; SPION-CCPM). $^{*}p<0.05$, $^{**}p<0.005$, $^{***}p<0.0005$, $^{****}p<0.0001$. Two-way ANOVA. Data represented as fold change (F.C.) vs. the non-treated condition (NT) unless otherwise indicated. For all, n = 3.

Supplemental figure 2

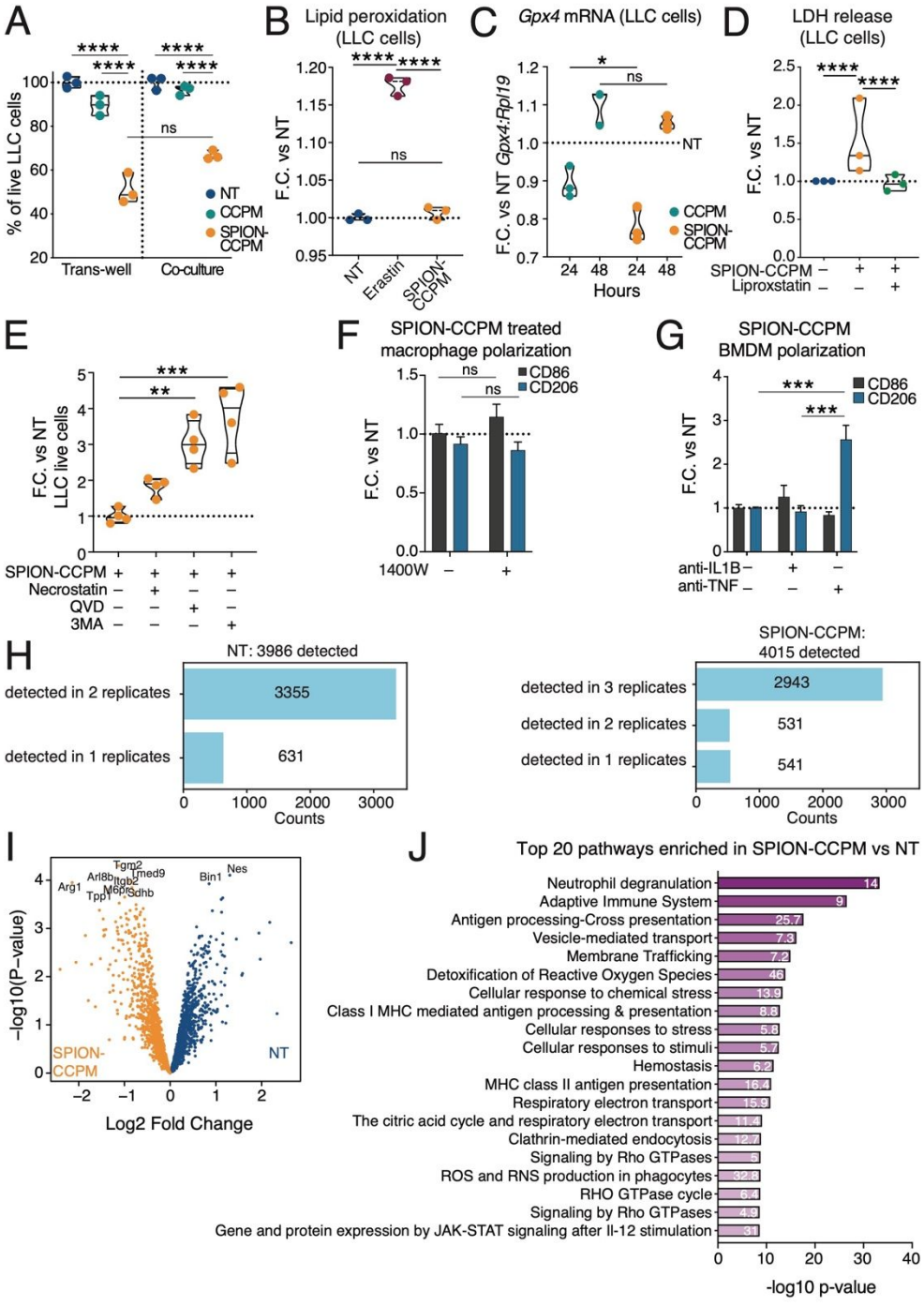

57 *Supplemental Figure 2: Secreted factors from SPION-CCPM-loaded macrophages induce cancer cell death*

(A) Viability of LLC cells following trans-well or co-culture (direct contact) with BMDMs and treatment with SPION-CCPMs, CCPMs or no treatment (NT) for 48 h. (B) Analysis of lipid peroxidation in co-cultured cancer cells treated with erastin, SPION-CCPMs, or no treatment (NT) after 24 h. (C) *Gpx4* mRNA levels in co-cultured LLC cells after treatment with SPION-CCPMs, CCPMS or NT. (D) Analysis of LDH levels in LLC cells co-cultured with BMDMs and treated with or without SPION-CCPMs or Liproxstatin for 48 h. (E) Quantification of live co-cultured LLC cells following treatment with SPION-CCPMs, Necrostatin, QVD or 3-methyl adenine (3MA) after 24 h. (F) Levels of CD86 and CD206 in SPION-CCPM-BMDMs after 48 h of treatment with 1400W. (G) Analyses of macrophage cell surface markers following SPION-CCPM treatment and inhibition of IL-1β or TNF for 72 h. Fold change (F.C.) vs SPION-CCPM treatment alone. (H) Bar diagrams showing how often proteins were quantified, based on LFQ intensities, in the samples belonging to each group. (I) Volcano plot displaying the differentially regulated proteins between NT and SPION-CCPM macrophages. (J) Top 20 Reactome pathways enriched in SPION-CCPM-treated vs non-treated (NT) BMDMs co-cultured with *Eml4-Alk* cells and identified by proteomic analysis. The enrichment scores are indicated. $^{*}p<0.05$, $^{**}p<0.005$, $^{***}p<0.0005$, $^{****}p<0.0001$ Two-way ANOVA. Data represented as F.C. vs the non-treated condition (NT) unless otherwise indicated. n = 3 per group. A, B, D, E) Samples measured by flow cytometry.

Supplemental figure 3

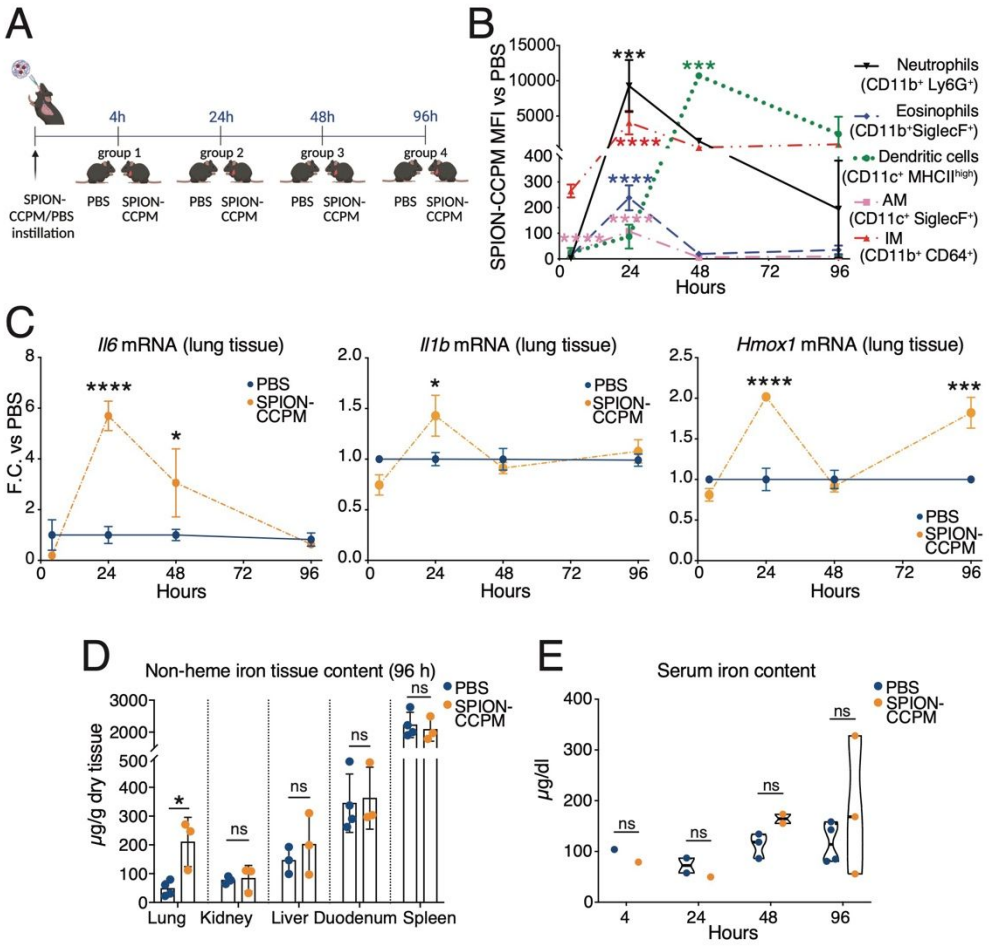

Supplemental Figure 3: SPION-CCPMs accumulate in various innate immune cell types and induce inflammation in WT mice

(A) Experimental design. (B) SPION-CCPM signal intensity measured by flow cytometry in innate immune cells of the bronchoalveolar lavage (BAL) for the indicated times. (C) mRNA expression analysis of *Il6*, *Il1b* and *Hmox1* genes in lung tissue. Data represented as fold change (F.C.) vs PBS mice. (D) Non-heme iron content in the specified organs at 96 h. (E) Serum iron content at 4, 24, 48 h (PBS n=3; SPION-CCPM n=2); 96 h (PBS n=4; SPION-CCPM n=3). *p<0.05, ***p<0.0005, Unpaired t-test (D) or Two-way ANOVA (B, C, E). n = 4 mice per group unless specified.

Supplemental figure 4

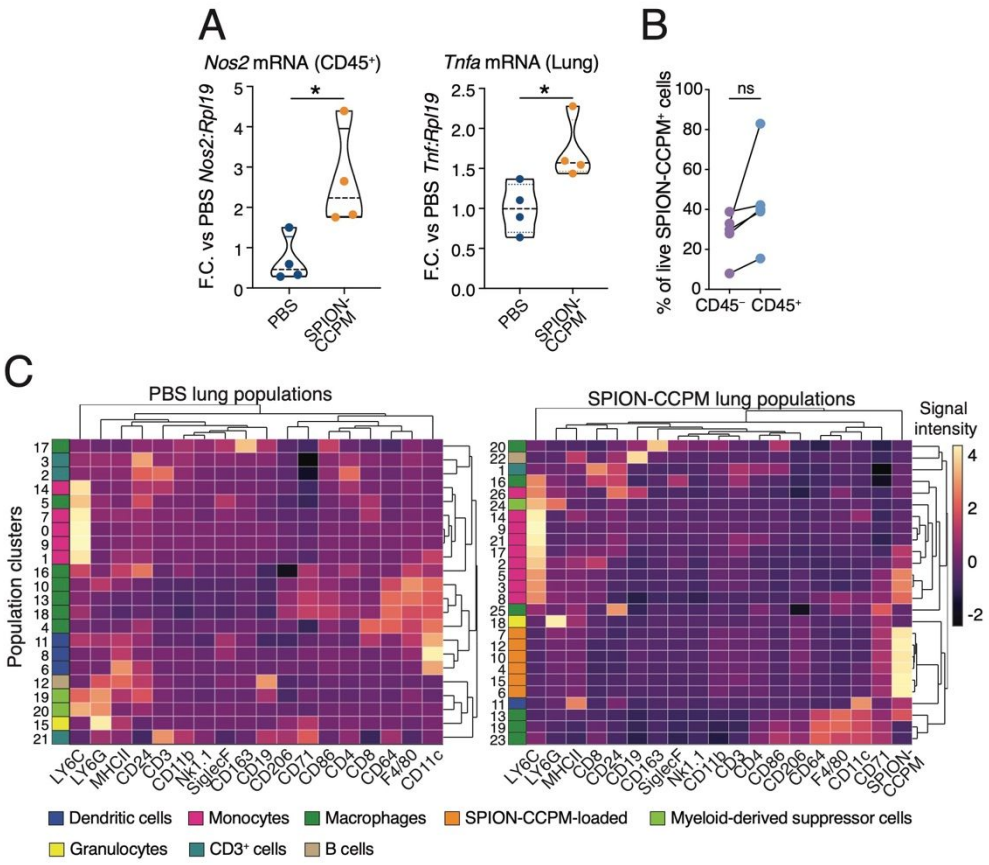

Supplemental Figure 4: Inflammation-induced alterations as a result of SPION-CCPM-treatment in Eml4-Alk mice

(A) *Nos2* and *Tnfα* mRNA levels in CD45$^+$ cells and total lung respectively; F.C. vs PBS mice. (B) Quantification of the frequency of population of SPION-CCPM$^+$ CD45$^-$ and CD45$^+$ lung cells by flow cytometry. (C) Heatmaps analysis of immune cells from lungs of PBS and SPION-CCPM treated mice. Cell surface markers (x-axis) measured by flow cytometry and clustered according to population likeness using the Phenograph algorithm (FlowJo), represented by population clusters (y-axis) and scaled by row. *p<0.05, Unpaired t-test (A, B).

94 *Supplemental Table 1:primer pairs for RT-PCR (Mus musculus)*

Gene	Sequence
Gclc	Forward 5' AGATGATAGAACACGGGAGGAG 3'
	Reverse 5' TGATCCTAAAGCGATTGTTCTTC 3'
Gpx4	Forward 5' CGCTCCATGCACGAATTCTC 3'
	Reverse 5' GCACACGAAACCCCTGTACT 3'
Hmox1	Forward 5' AGGCTAAGACCGCCTTCCT 3'
	Reverse 5' TGTGTTCCTCTGTCAGCATCA 3'
Il-1β	Forward 5' TCCGTGCAGACATTGTGGAG 3'
	Reverse 5' CTGCTTCTCAAAGTCAGGGTTG 3'
Il-6	Forward 5' GCTACCAAACTGGATATAATCAGGA 3'
	Reverse 5' CCAGGTAGCTATGGTACTCCAGAA 3'
Nos2	Forward 5' TGGAGACTGTCCCAGCAATG 3'
	Reverse 5' CAAGGCCAAACACAGCATACC 3'
Nqo1	Forward 5‘ AGCGTTCGGTATTACGATCC 3'
	Reverse 5‘ AGTACAATCAGGGCTCTTCTCG 3'
Rpl19	Forward 5' AGGCATATGGGCATAGGGAAGAG 3'
	Reverse 5' TTGACCTTCAGGTACAGGCTGTG 3'
Tnfα	Forward 5' TGCCTATGTCTCAGCCTCTTC 3'
	Reverse 5' GAGGCCATTTGGGAACTTCT 3'

95

Supplemental Table 2: flow cytometry antibodies (Mus musculus)

Antibody	Fluorophore	Clone	Isotype	Manufacturer
CD11b	PerCP	ICRF44	N/A	ThermoFisher
CD11c	PE	N418	N/A	BioLegend
CD11c	Brillant Violet 650	117339	NA	Biolegend
CD163	Pe-Cy7	25-1631-82	NA	Life Technologies
CD19	PE	115508	NA	Biolegend
CD206	Alexa Fluor 700	MR6F3	Rat IgG2b, κ	ThermoFisher
CD206	FITC	141704	NA	Biolegend
CD24	Super Bright 436	62-0242-80	NA	Life Technologies
CD3	Alexa Fluor 700	100215	NA	Biolegend
CD326	Alexa Fluor 594	118222	NA	Biolegend
CD4	Brillant Violet 570	100541	NA	Biolegend
CD45	PerCP-Cy5.5	104	N/A	ThermoFisher
CD64	Brillant Violet 711	X54-5/7.1	N/A	BioLegend
CD71	Brillant Violet 510	RI7217	Rat IgG2a, κ	BioLegend
CD8	Pe-Cy5.5	SBA-1550-16	NA	Biozol
CD86	Brillant Violet 421	GL-1	Rat IgG2a, κ	BioLegend
CD86	Brillant Violet 785	105043	NA	Biolegend
F4/80	Brillant Violet 605	T45-2342	N/A	ThermoFisher
Ly6C	PE-Dazzle	HK1.4	N/A	BioLegend
Ly6G	FITC	1A8	N/A	BioLegend
Ly6G	Brillant Violet 605	127639	NA	Biolegend
MerTK	Brillant Violet 421	108928	Rat IgG2a	ThermoFisher
MHC II	Pe-Cy7	M5/114.15.2	Rat IgG2b, k	Biolegend
MHC II	Alexa Fluor 532	58-5321-82	NA	Life Technologies
Nk1.1	APC-Fire 810	156519	NA	Biolegend
Siglec-F	APC-Cy7	E50-2440	N/A	ThermoFisher